Effects of surface impurities on surface diffusion of CO on Ni(110)

Xudong Xiao
Department of Physics, Hong Kong University of Science and Technology, Hong Kong, China

Yuanlin Xie, Christian Jakobsen, and Y. R. Shen
Department of Physics, University of California, Materials Sciences Division, Lawrence Berkeley National Laboratory, Berkeley, California 94720

(Received 27 February 1997)

A small amount of coadsorbed impurity species could significantly alter the surface diffusion of CO on Ni(110). Three impurity species, sulfur, oxygen, and potassium are studied here. The former two are known as ''poisons'' and the latter as a ''promoter'' for CO hydrogenation on Ni. All three are found to impede CO diffusion drastically. The apparent diffusion activation energy E_D increases from the clean-surface value of 2–3 kcal/mol, to a saturation value of 7–8 kcal/mol at sufficiently high impurity coverages. The impeding effect decreases from S to O to K. Mechanisms responsible for the effect are discussed in detail. With S and O, the impurity-covered step-controlled diffusion appears to be the dominant mechanism. With K, the nearest-neighbor attractive interaction between CO and K seems to be most important. [S0163-1829(97)01944-9]

I. INTRODUCTION

Surface diffusion is one of the most important subjects in surface science due to its relevance to crystal growth and surface catalysis. It has been studied extensively.[1] Surface impurities or surfactants may have strong influences on surface diffusion. Oxygen, for example, was found to reduce the Schwoebel energy barrier at step sites for Pt self-diffusion on Pt(111), and therefore to improve the epitaxial growth of the crystal.[2] Small amounts of sulfur and oxygen were found to poison, and potassium to promote, surface-catalyzed CO hydrogenation reactions.[3] Surface diffusion as an intermediate step in catalysis may bear the impurity effect, and must be investigated.

The impurity effect may also have contributed to the inconsistent experimental results of nominally the same systems obtained by different groups. For example, CO diffusion on Pt(111) was measured by five groups with different methods, and the reported diffusion coefficients at a given temperature differed by as much as four orders of magnitude.[4] A similar situation exists for H/Ni(100) and for other systems.[5] Both the deduced activation energy and preexponential factor are very different.[4,5] Although suggestions based on the difference in measurement methods and other effects were made to explain the inconsistency qualitatively,[6] the effect of impurity on the samples was never examined.

For surface self-diffusion, earlier studies found both enhancement and impediment effects from different impurities.[7–9] For W self-diffusion studied with field-emission technique,[7,8] a monolayer of metallic Pd or Ni could reduce the activation energy by as much as 30 kcal/mol (from 74 to 44 kcal/mol), and enhance the diffusivity by about two orders of magnitude, while half of a monolayer of C or O could raise the activation energy barrier by as much as 126 kcal/mol (from 74 to 200 kcal/mol), and decrease the diffusivity by more than one order of magnitude at the relevant measurement temperatures. Similar studies were conducted for Cu and Ag self-diffusion, with similar results.[9] While most of these studies involved a large amount of impurity, a few with low coverages were found not to alter the self-diffusivities. For instance, ~0.1-ML C was found not to affect the W self-diffusion at all.[8] One might expect that the same could be true for heterogeneous surface diffusion. However, measurements have indicated a fairly strong impurity effect in this case. A few percent of a monolayer of C were found to increase the Pb diffusion coefficient on a stepped surface around W(100) by as much as ten orders of magnitude.[10] In the case of C and S impurities on Ru(100),[11] 0.1 ML was found to impede H diffusion by a factor of ~6. Clearly, a small amount of impurities could not be neglected in the case of heterogeneous surface diffusion.

Although experimental data were limited, usually to 1–2 temperatures only,[10,11] two types of models were proposed in the past to explain the observed impurity effect for heterogeneous surface diffusion. The first one suggested that impurities modify special surface sites, namely, step sites, and therefore change the measured overall diffusion coefficient.[10] The second one assumed ''long-range'' interaction between impurities and diffusing species, such as a ''long-range'' blocking effect, on the normal terraces in order to explain the observed strong impurity coverage dependence—a non-negligible effect even at very low coverages (~0.01 ML).[11]

We recently reported on the effect of S impurities on surface diffusion of CO on Ni(110), and identified S-modified step-controlling diffusion as responsible for our observation.[12] In this paper, we will first present our experimental results of the impurity effect to include impurities O and K, in addition to S. The CO coverages investigated are $\theta_{CO} \sim \theta_{Sat}$ and $\theta_{CO} \sim 0.5$ ML. The results clearly show that all three elements impede CO diffusion strongly, with a decreasing strength from S to O to K. The S effect is so strong that 0.02 ML of S on a high-temperature-annealed surface can increase the diffusion activation energy E_D along [110] from its clean surface value of 2.2 kcal/mol to 7.4 kcal/mol, for example. To reach a similar effect, more oxygen or potassium is required. Although all three elements impede CO

diffusion by increasing the apparent activation energy E_D, the mechanisms are different. Sulfur and oxygen seem to affect CO diffusion through their modification of steps on the Ni(110) surface, leading to step-controlling surface diffusion for CO, but potassium seems to affect CO diffusion through a CO-K interaction. For a CO coverage $\theta_{CO} \sim 0.5$ ML, the saturation of E_D begins at a smaller impurity coverage than the case of $\theta_{CO} \sim \theta_{Sat}$. This can be explained by the effect of a CO-CO interaction on surface diffusion.

II. EXPERIMENT

A. Measurement technique

The experimental technique we used to study surface diffusion is a linear optical diffraction method that has been described in detail elsewhere.[13,14] We summarize the key points here. First, a monolayer or prescribed submonolayer of CO was deposited on the Ni(110) surface. Then a one-dimensional grating of adsorbates was created by interfering two laser beams [Nd:YAG (yttrium aluminum garnet) laser at 1.06 μm] at the surface via-laser induced thermal desorption (LITD). To avoid complication in data analysis due to the coverage dependence of the diffusion coefficient, the grating depth was made as shallow as possible, usually limited by the detection signal-to-noise ratio. In the present case, it was typically $\sim$0.03 ML. This was obtained by properly adjusting the intensities of the two interfering laser beams such that $\sim$0.03 ML CO was desorbed from the maximum laser intensity regions, and no CO desorbed from the minimum intensity regions.[13] As determined by the laser interference pattern, the grating spacing was 3 μm in the present experiment.

The adsorbate grating could be detected by linear diffraction of a He-Ne laser beam. If the grating is smeared out by surface diffusion, the diffraction signal should exhibit an exponential decay in time:[13,14]

$$S(t) = S(0)\exp(-t/\tau) \quad \text{with} \quad \tau = s^2/8\pi^2 D, \qquad (1)$$

where D is the chemical diffusion coefficient and s is the grating period. In the present study, D was measured as a function of substrate temperature and surface impurity coverage.

We note that simple linear diffraction off a monolayer grating normally would result in a very small signal buried in a strong background arising from light scattering from the substrate. With a polarization modulation technique, however, the background could be greatly suppressed, allowing the weak diffraction signal to be detected.[14] This modulation method utilized the fact that the adsorbed CO molecules respond more strongly to p-polarized light than to s-polarized light, while the scattering background does not have such a polarization dependence. An improvement of five orders of magnitude in the signal-to-background ratio can be readily achieved.

B. Sample preparation

The experiment was performed with the sample situated in an ultrahigh-vacuum (UHV) chamber that had a base pressure of 2.0×10^{-10} torr. A single crystal of Ni(110), cut and mechanically polished to within 0.2° of the (110) plane (the miscut steps are in the direction about 25° from $[1\bar{1}0]$), was used in our measurements. Extensive cycles of Ar^+ sputtering and high-temperature annealing of the crystal were first carried out to obtain a well-ordered surface. The routine cleaning procedure of the Ni surface was to Ar^+ sputter the surface at room temperature for 30 min, followed by annealing at 1120 K for 10 min, a slow cooling of $\sim$0.5 K/s to 800 K, and then a more rapid cooling of $\sim$2 K/s to room temperature. Auger spectra of the clean surface showed no detectable impurities ($<$0.5% S and C, and $<$1% O). Observation of a sharp 1×1 low-energy electron diffraction (LEED) pattern from a clean Ni(110) surface and a 2×1 pattern from a full CO monolayer on Ni(110) ensured that the surface was well ordered. The sample temperature was monitored by a thermocouple and controlled to within ±1 K.

To deposit sulfur on Ni(110), H_2S gas was leaked into the UHV chamber, followed by adsorption and dissociation of H_2S on Ni(110). Flashing the sample to 570 K desorbed the hydrogen, leaving only S on the surface.[15] A second method to prepare S on the Ni(110) surface was by heating the sample at 1120 K for an extended period, usually on the order of hours, to segregate S from the bulk to the surface. The amount of sulfur appearing on the surface could be measured by Auger-electron spectroscopy (AES) calibrated against the saturation coverage 0.67 ML of sulfur that has a $p(3\times2)$ LEED structure at room temperature.[15,16]

Deposition of oxygen on Ni(110) was by leaking O_2 gas into the UHV chamber. The O_2 molecules adsorbed and dissociated on Ni(110) at room temperature. Flashing the substrate to $>$400 K was necessary in order to make the adsorbates thermally equilibrated with the surface, because oxygen adsorbed at room temperature was kinetically limited to nonequilibrium states.[17] Oxygen coverage was determined from AES and LEED measurements. The brightest 3×1, 2×1, and 3×1 reconstructions observed in sequence by LEED corresponded to $\frac{1}{3}$, $\frac{1}{2}$, and $\frac{2}{3}$ ML of oxygen coverages, respectively.[16,18] With the calibrations by LEED, the AES ratio of O(512)/Ni(848) was used as a measure of the oxygen coverage. Possible loss of oxygen due to formation of CO_2 by reaction with CO was less than 1% of the predosed oxygen (with $\theta_O < 0.20$ ML), consistent with those reported by others.[19]

Potassium was deposited on Ni(110) by heating a surface activated emission source (SAES) getter (a commercial dispenser) in the UHV chamber with an electrical current of about 7–9 A, depending on the remaining amount of K in the dispenser. The K coverage was measured by the AES ratio of K(252)/Ni(848), calibrated by the saturation coverage of 0.50 ML.[20,21] In order to ensure that only 1 ML of potassium could adsorb on the surface at saturation, the substrate was kept at a temperature $\sim$30 K higher than the room temperature.[21]

With the chosen impurity, S, O, or K, preadsorbed on the Ni(110) surface at a known coverage, we then dosed the surface with CO at 160 K to a half or full monolayer coverage. The sample temperature was subsequently raised or lowered to the diffusion temperature before creating the CO grating by laser desorption. Since CO would be thermally desorbed at a much lower temperature than any of the above three impurities, LITD would have little effect in desorbing the impurities. Once the grating was formed, the first-order

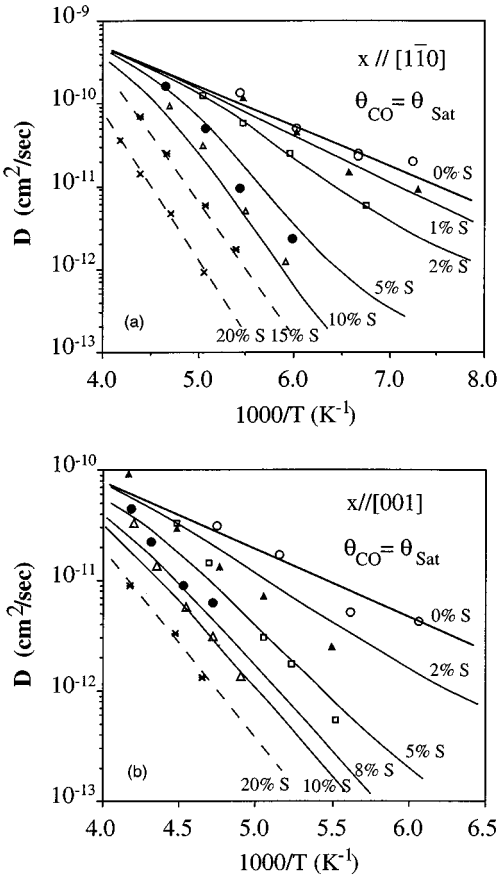

FIG. 1. CO diffusion coefficient D vs reciprocal temperature $1/T$ along (a) [1$\bar{1}$0] and (b) [001] for a number of preadsorbed S coverages as labeled. The solid lines are theoretical fits, and the dashed lines at higher S coverages are a guide for the eye. The CO coverage corresponds to a saturation monolayer.

diffraction signal from the grating would be measured as a function of time, as we discussed earlier.

III. EXPERIMENTAL RESULTS

Here we present experimental results on how S, O, and K as surface impurities affect CO diffusion on Ni(110). In a previous short communication,[12] the effect of S on CO diffusion at saturation CO coverage was described. These results will be included here for completeness. They are presented in Figs. 1(a) and 1(b), showing D versus $1/T$ for CO diffusion along [1$\bar{1}$0] and [001], respectively, for several S impurity coverages prepared by H_2S dosing. It is obvious from Fig. 1 that CO diffusion is strongly impeded by the presence of sulfur, and is more so in the low-temperature regime. The effect is already significant at an S coverage of $\theta_S=0.01$ ML. Fitting the data to the Arrhenius form, $D=D_0\exp(-E_D/kT)$, yields the diffusion activation energy E_D and the preexponential factor D_0. The deduced E_D and D_0 versus θ_S is depicted in Fig. 2 for CO diffusion along [1$\bar{1}$0] [Figs. 2(a) and 2(b)] and along [001] [Fig. 2(c)], respectively. Note that E_D increases monotonically from the clean surface value of 2.2 ± 0.3 kcal/mol to a saturation value of 7.4 ± 0.5 kcal/mol at $\theta_S\sim0.10$ ML for CO diffusion along

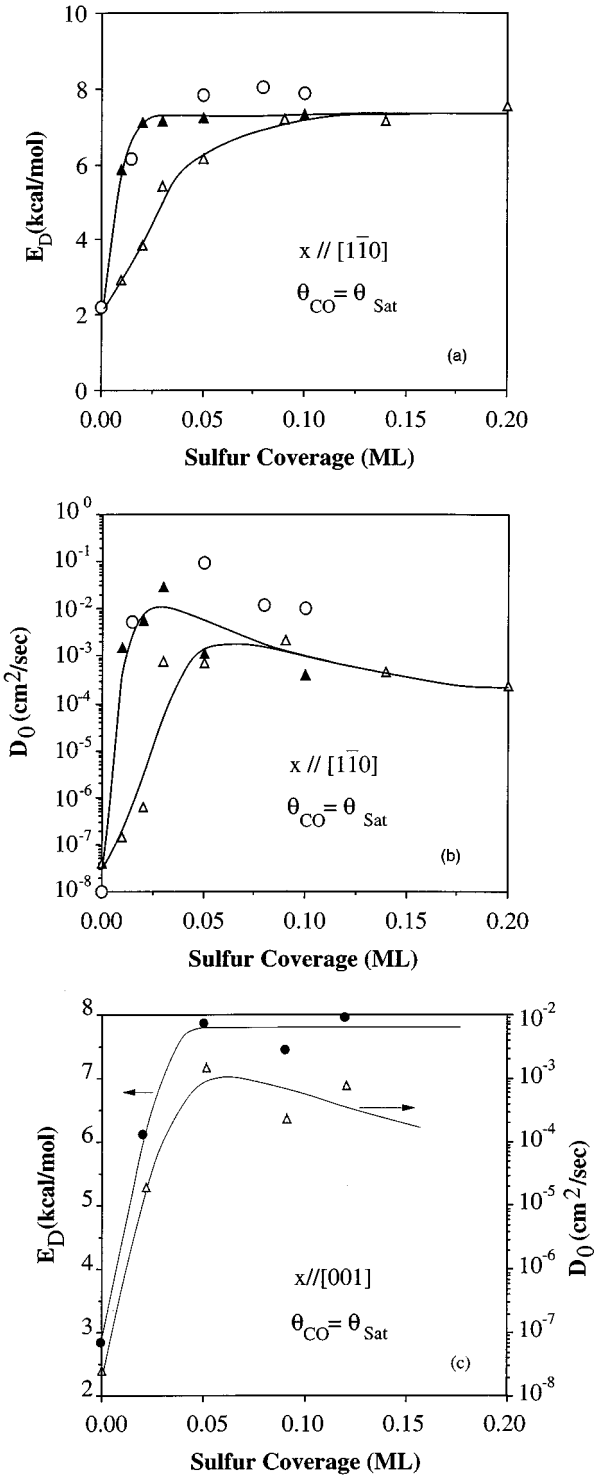

FIG. 2. Apparent diffusion activation energy E_D and preexponential factor D_0 for CO diffusion along [1$\bar{1}$0] [(a) and (b)] and [001] (c) as a function of sulfur impurity coverage. The solid lines are a guide for the eye. The open and filled triangles in (a) and (b) are obtained from samples without and with annealing at 1120 K for 12 min, respectively, after H_2S dosing. The open circles are obtained from samples with S segregated from the bulk. The CO coverage corresponds to a saturation monolayer.

[1$\bar{1}$0], and from 2.8 ± 0.3 kcal/mol to 7.8 ± 0.5 kcal/mol at $\theta_S\sim0.05$ ML along [001]. Further decrease of D observed with increasing θ_S comes from a decrease of D_0 only.

When the S impurity coverage on Ni(110) was prepared

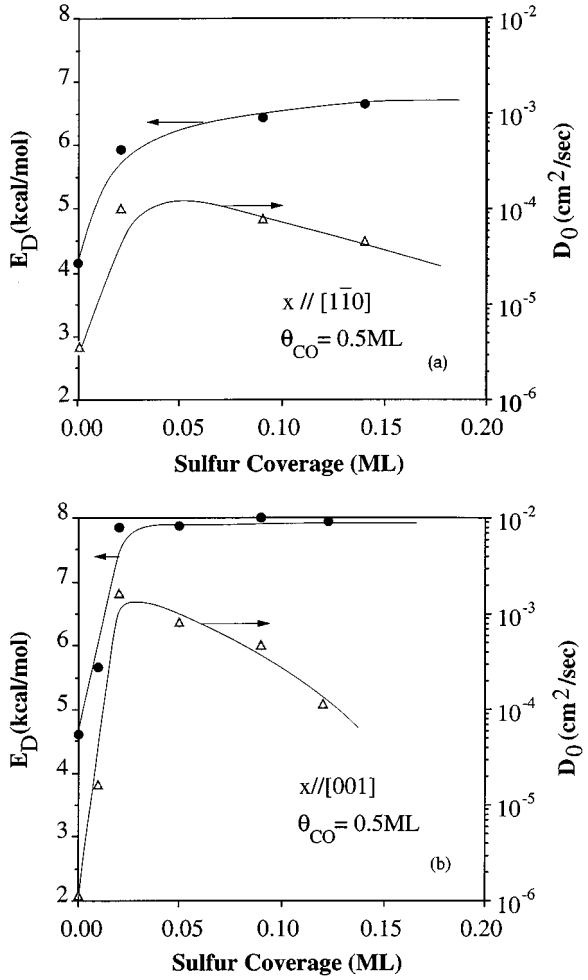

FIG. 3. Apparent diffusion activation energy E_D and preexponential factor D_0 for CO diffusion along (a) [110] and (b) [001] as a function of sulfur impurity coverage. The solid lines are a guide for the eye. The CO coverage corresponds to $\theta_{CO}\sim 0.5$ ML.

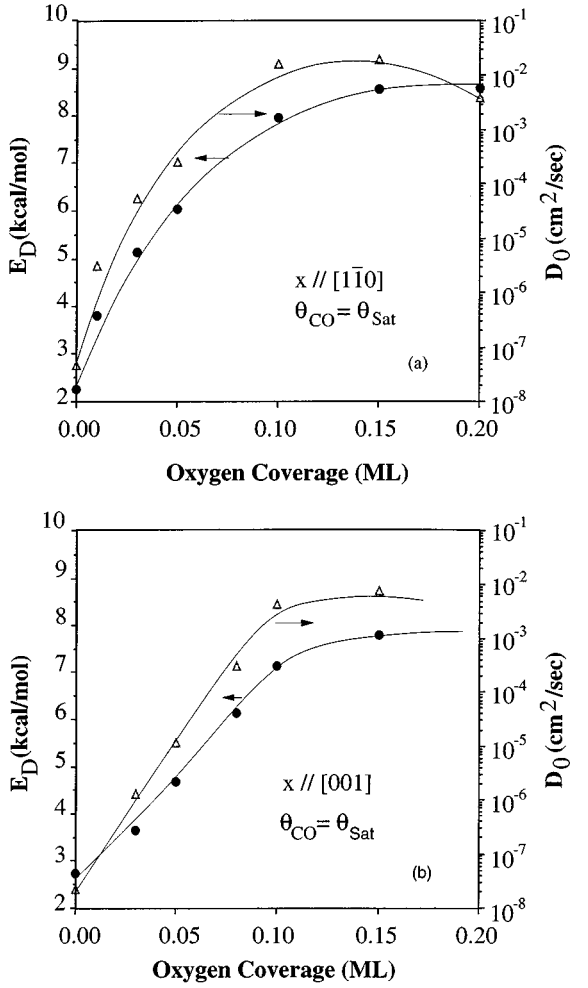

FIG. 4. Apparent diffusion activation energy E_D and preexponential factor D_0 for CO diffusion along (a) [110] and (b) [001] as a function of oxygen impurity coverage. The solid lines are a guide for the eye. The CO coverage corresponds to a saturation monolayer.

by bulk segregation through heating, its effect on CO diffusion along [110] was found to be much stronger. As displayed in Fig. 2(a), E_D already reaches 6.2 kcal/mol at $\theta_S\sim 0.01$ ML, as compared to 2.8 kcal/mol in the previous case, and approaches the saturation value of 7.5 kcal/mol at $\theta_S\sim 0.02$ ML. The difference between this and the previous case came from high-temperature annealing of the sample. The same strong impurity effect was observed if the sample with S coverage prepared by H_2S deposition was annealed at 1120 K for 2–12 min. This is also presented in Fig. 2(a). Auger electron spectroscopy indicated that the S coverage was not affected by annealing. For CO diffusion along [001], however, no significant difference between different ways of sample preparation was found. Thus high-temperature annealing must have changed the surface structure of Ni(110) in such a way that it mainly modifies CO diffusion along [110].

Measurement of the effect of sulfur impurity was also carried out at a half-monolayer CO coverage: $\theta_{CO}\sim 0.5$ ML. The activation energy and preexponential factor, E_D and D_0, deduced from the measured D versus $1/T$, are presented in Figs. 3(a) and 3(b) for CO diffusion along [110] and [001], respectively. The same behavior as in the case of saturation CO coverage is found except that the saturation of E_D now appears at an even lower S coverage: at $\theta_S\sim 0.05$ ML for CO diffusion along [110], and $\theta_S\sim 0.02$ ML along [001]. The saturation value of E_D is somewhat smaller along [110] (6.5 ± 0.5 kcal/mol instead of 7.4 ± 0.5 kcal/mol) but remains the same along [001].

The effect of oxygen impurity on CO diffusion on Ni(110) is shown in Figs. 4 and 5 for $\theta_{CO}\sim\theta_{Sat}$ and $\theta_{CO}\sim 0.5$ ML, respectively. In the figures, E_D and D_0 deduced from measured D versus $1/T$ for diffusion along both [110] and [001] directions are plotted against the oxygen coverage. Qualitatively, the behavior is similar to the S impurity case. There is, however, a quantitative difference in the impurity coverage dependence and saturation values of E_D. For $\theta_{CO}\sim\theta_{Sat}$, E_D reaches a saturation value of 8.5 ± 0.5 kcal/mol for CO diffusion along [110], and 7.9 ± 0.5 kcal/mol along [001] at an oxygen coverage $\theta_O\sim 0.15$ ML. For $\theta_{CO}\sim 0.5$ ML, the saturation occurs at a smaller oxygen coverage, $\theta_O\sim 0.10$ ML, which is again similar to the S impurity case, with a saturation value of E_D of 7.8 ± 0.5 kcal/mol along [110], and 7.4 ± 0.5 kcal/mol along [001].

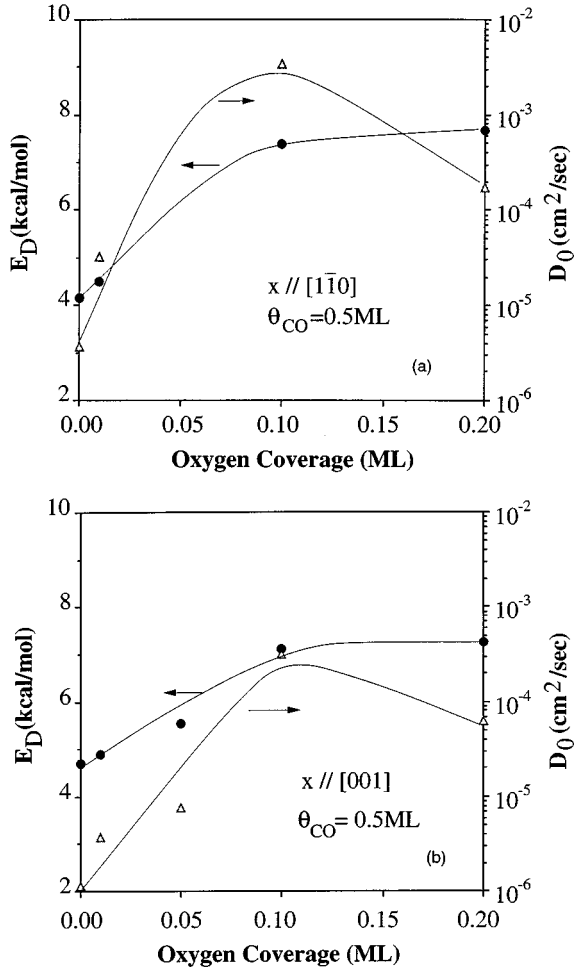

FIG. 5. Same as Fig. 4, except the CO coverage corresponds to θ_{CO}~0.5 ML.

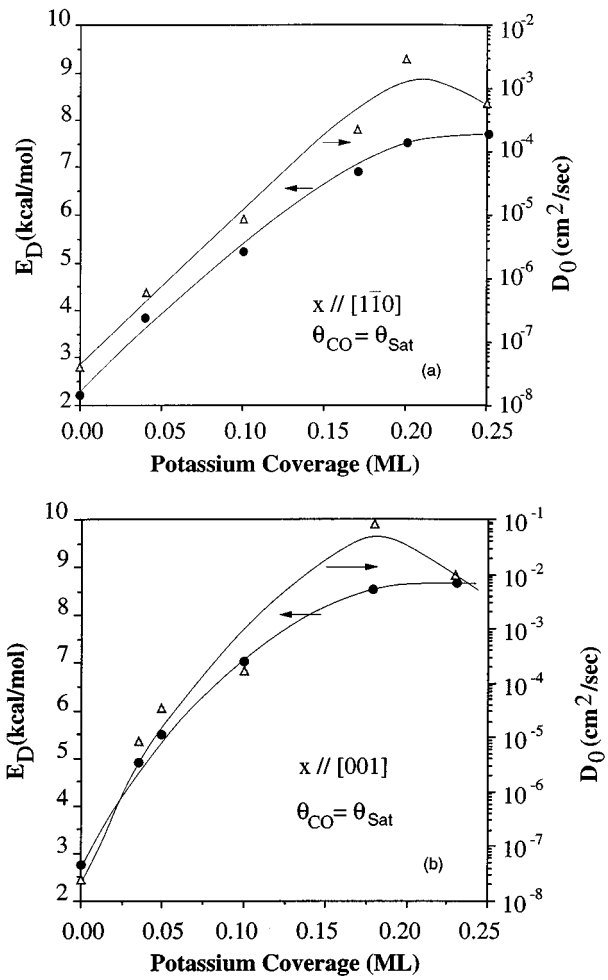

FIG. 6. Same as Fig. 4, with the horizontal axis replaced by potassium coverages.

Potassium has the least effect on CO diffusion on Ni(110) among the three impurities. Figures 6(a) and 6(b) show E_D and D_0 versus potassium coverage θ_K for CO diffusion along [1$\bar{1}$0] and [001], respectively, at saturation CO coverage. Again, a behavior similar to that found with S and O impurities is observed, with a difference only in the quantitative aspect of the impurity coverage dependence. The activation energy E_D now saturates at θ_K~0.20 ML, with saturation values of 7.7±0.5 and 8.5±0.5 kcal/mol for CO diffusion along [1$\bar{1}$0] and [001], respectively.

The preexponential factor D_0 for all cases first increases with the impurity coverage. This seems to be the result of a compensation effect to the increase of E_D with impurity coverage. It then reaches a maximum as E_D approaches saturation. Further increase of impurity coverage results in a decrease of D_0.

IV. DISCUSSION

A. CO diffusion on S-preadsorbed Ni(110)

We have found that the results of CO diffusion on a S-preadsorbed Ni(110) surface can be understood by a S-modified step-controlled diffusion model.[12] Any other models inevitably lead to disagreement with the experimental data. Here we discuss how we reached this conclusion.

Consider first an ideal Ni(110) surface with no step defects. For low S coverage, the S atoms are adsorbed at the twofold hollow sites of the Ni(110) surface, forming a full $c(2\times2)$ overlayer at 0.50-ML coverage.[16] Higher S coverage can result in compression of the S overlayer to $p(3\times2)$ at saturation coverage at room temperature.[15,16] No surface reconstruction induced by S has been observed. The binding between S and Ni is so strong that the S atoms do not desorb from the surface even at 1200 K.[22] However, they diffuse readily on the surface at sufficiently high temperatures. For example, under our sample preparation conditions, with the sample finally flash annealed at 570 K, S atoms should reach their thermal equilibrium positions on the surface and then remain stationary when the sample is cooled to 240 K or lower for CO diffusion measurements. This is seen from the known activation energy barrier of 15–28 kcal/mol and diffusivity of $\sim10^{-12}$ cm^2/s at 500 K for S diffusion on Ni field emitters.[22] The maximum diffusivity is less than 10^{-19} cm^2/s at 240 K. The above picture is confirmed by scanning tunneling microscopy STM studies showing that S at low coverages diffuses readily on Ni(110) even at room temperature and tends to end up at step sites.[23]

Coadsorption of S and CO would have S adsorbed at the twofold hollow sites, and CO at the short-bridge sites. However, although no direct quantitative study of CO and S coad-

sorption on a Ni(110) surface has been reported, studies on Ni(100) (Ref. 24) and Ni(111) (Ref. 25) allow us to conclude that preadsorbed S has two effects on CO adsorption: one is that each S on a twofold hollow site sterically blocks two neighboring short-bridge CO sites. This reduces the saturation CO coverage. The other is that the CO molecules adsorbed at the next-nearest-neighbor sites of an adsorbed S are pushed away from their normal binding positions to some extent, and accordingly their CO-Ni binding strength is weakened. The STM images of coadsorbed S and CO on Ni(110) at low S coverages actually showed segregation of the two adsorbates with a S island size of ~50 Å.[23] This confirms the repulsive interaction between S and CO, and is consistent with results of our thermal-desorption spectroscopy measurement. As a consequence, the number of S-affected CO molecules in the next-nearest-neighbor sites is also reduced.

The repulsive interaction between S and CO has a tendency to make the CO molecules diffuse away from S. Therefore, in the S-infected neighborhood CO molecules would have a lower diffusion energy barrier. Thus a decrease of effective activation energy E_D versus S coverage would be expected.[26,27] This is in contradiction to our observation.

It is possible that, to avoid the S-affected sites, CO takes a detour path in diffusion. If the detour is too long, then CO may rather diffuse directly through the S-affected areas. This is likely to happen only at high S coverages. Such a model can qualitatively explain the observed increase of E_D versus θ_S, but quantitative agreement cannot be obtained. A simulation by Brand and co-workers[11] showed that, for H diffusion on Ru(001), 0.10 ML of S slows down the diffusion only by a factor of 6, even with the assumptions of a ''long-range interaction'' that each S can block ten neighboring adsorption sites of H, and that the energy barrier at the blocked sites is infinite. Their result is applicable to our case. If the energy barrier in the S-affected areas is not infinite, the reduction of the CO diffusion coefficient is even smaller, and is certainly too small to explain our observation. For example, we observed that the CO diffusion at $T \sim 180$ K is slowed down by a factor of ~50 by 0.10 ML of S on Ni(110). At lower temperatures, the reduction is even greater. A much larger influence circle of S, i.e., much more than ten neighboring CO adsorption sites, would be needed to explain the observed result using this model. This is contradictory to all theoretical predictions that the effect of S on a substrate surface cannot extend beyond its next-nearest neighbors (~10 CO sites).[28] One may suggest that a mobile S can effectively affect more CO molecules on a surface than a stationary one, but as mentioned earlier, at our measurement temperatures the S atoms are basically stationary. Even if S is mobile, the temperature dependence of CO diffusion would be wrong since the higher mobility of S at higher temperatures would lead to a stronger reduction of the CO diffusion coefficient, opposite to what we observed.

We now consider a Ni(110) surface with steps. Even on a sample with a surface misorientation of $<0.2°$, as was the case with our sample, steps are expected to have a density of ~1 step/500 Å. The S impurities at thermal equilibrium preferentially occupy the step sites.[23] They line up along the steps and create a higher-energy barrier for CO to cross the steps. This then results in the step-controlled surface diffusion. Our STM images showed no other peculiar structures on the Ni(110) surface in the range of S coverage we investigated.

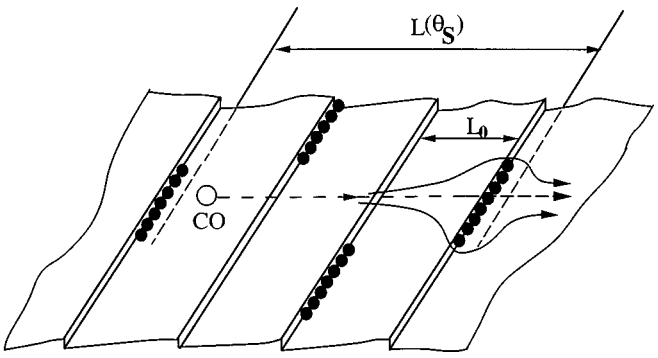

FIG. 7. Schematic showing CO diffusion on a stepped surface, with the steps partially covered by impurities.

We now discuss the step-controlled surface diffusion model in some detail. In this model, we assume the following. (i) Only S atoms at the step sites are effective in blocking CO diffusion, which is certainly true for low S coverages. (ii) The diffusion energy barrier on terraces is not affected by S impurities, but at the S-modified steps, it has a constant value E_s. (iii) CO molecules can diffuse over an S-covered step site either directly by crossing the high-energy barrier or indirectly by taking a detour around the S-covered part of the step. (The unoccupied step site is assumed to have the same barrier height around it as the terrace sites.[29]) (iv) The S atoms aggregate along the steps and form segments. With these assumptions, the macroscopic diffusion coefficient D can be derived following Fig. 7 and the relation $\langle x^2 \rangle = 2Dt$. We find

$$\frac{1}{D} = \frac{[L(\theta_S) - a]^2}{L^2(\theta_S) D_t} + \frac{a^2}{L^2(\theta_S) D_s}, \tag{2}$$

where a is the lattice constant along the diffusion direction, D_t and D_s are the diffusion coefficients for diffusion on terraces and over S-controlled steps, respectively. The first term here accounts for diffusion between two adjacent S-modified steps and the second term for diffusion across a S-modified step. The average spacing between two neighboring S-covered steps is given by $L(\theta_S) = L_0 / \gamma\theta_S$, where L_0 is the average terrace width and $\gamma\theta_S$ is the fraction of step sites covered by S at θ_S. Since there are two parallel channels for diffusing over a S-modified step, one directly crossing the step and the other making a detour around the step, the corresponding diffusion coefficient is given by

$$D_s = D_I + (1 - \gamma\theta_S)^2 D_{II}, \tag{3}$$

with $D_I = D_{I0} \exp(-E_s/kT)$ describing diffusion through the first channel and $(1 - \gamma\theta_S)^2 D_{II}$ through the second channel. The heuristic argument for choosing the latter expression is as follows: At coverage θ_S of S, the probability for a step site occupied by S is $\gamma\theta_S$, and that for a step site unoccupied is $1 - \gamma\theta_S$. The average length of a S-covered step is then given by $a/(1 - \gamma\theta_S)$. The average time for CO to diffuse over the step by detour is $a^2/(1 - \gamma\theta_S)^2 2D_t$ following the diffusion relation $\langle x^2 \rangle = 2Dt$. Considering that a is the effective diffusion length in the process, we would find the

effective diffusion coefficient to be $(1-\gamma\theta_S)^2 D_t$. However, such a model neglects possible changes of CO coverage along the step from the average one. We then simply replace D_t by D_{II}, which has the same activation energy as D_t but a different preexponential factor that can be used as an adjustable parameter in our data fitting.

As already discussed in detail in Ref. 12, D_t and D_I in Eqs. (2) and (3) can be determined from measurements at $\theta_S=0$ and $\gamma\theta_S=1$ (with $\theta_S=0.10$ ML), and L_0 can be deduced from the STM measurement.[30] For our sample, we find $D_t=4.4\times10^{-8}\exp(-2.2\ \text{kcal mol}^{-1}/kT)$ cm^2/s and $(L_0/a)^2 D_I=2.4\times10^{-3}\exp(-7.4\ \text{kcal mol}^{-1}/kT)$ cm^2/s along [110] and $D_t=2.2\times10^{-8}\exp(-2.8\ \text{kcal mol}^{-1}/kT)$ cm^2/s and $(L_0/a)^2 D_I=1.7\times10^{-4}\exp(-7.4\ \text{kcal mol}^{-1}/kT)$ cm^2/s along [001]. We can then use Eqs. (2) and (3) to fit the data in Fig. 1 by taking $D_{II}=D_{II0}\exp(-E_t/kT)$ with $E_t=2.5$ kcal/mol being an average of $E_t(110)$ and $E_t(001)$, and treating D_{II0} as the only adjustable parameter. In Fig. 1, the solid curves that fit the data are obtained with $D_{II0}=7.0\times10^{-15}$ cm^2/s. The agreement between theory and experiment appears quite satisfactory. For $\theta_S>0.10$ ML, we have not attempted to fit the data with our model because the high density of S impurities on the terraces may now have an appreciable effect on D_t, as suggested by Mak *et al.*[11]

We note that, although the above picture of impurity-affected step-controlled diffusion includes all the necessary ingredients, the quantitative aspect of the theory may not be very correct because of the assumptions involved in deriving Eq. (2). For example, as suggested by Ying, the correct equation should have a weaker dependence on the terrace width than the square dependence we choose.[31]

The stronger impurity effect seen with S segregated from bulk or with high-temperature annealing of the sample can also be explained by the S-modified step-controlled model.[12] Our STM measurement shows that steps on the Ni(110) sample surface with S impurities undergo a morphology change after high-temperature annealing. The original steps along the surface-miscut direction disappeared, and were replaced by ~5 steps/μm along diagonal directions (i.e., [111] and [111]) of the surface unit cell, plus additional ones (10 steps/μm) along [110]. The observed saturation of E_D along [110] at a lower S coverage of $\theta_S\sim0.02$ ML, as compared to $\theta_S\sim0.10$ ML before annealing, indicates that S must have adsorbed at these diagonal steps more readily to ensure all these step sites covered by S at $\theta_S\sim0.02$ ML. With the effective terrace width along [110] basically unchanged (within our statistical error of 15% from step counting) in spite of the step morphology change, CO diffusion along [110] could now be controlled by the S-covered steps at $\theta_S\sim0.02$ ML. For diffusion along [001], however, the average terrace width is significantly larger so that the S-covered diagonal steps were not yet sufficient to dominate the CO diffusion. In order to reach the step-controlled diffusion limit, steps along [110] must also be covered by S, but this could happen only at $\theta_S\sim0.10$ ML.

B. CO/O on Ni(110)

Because oxygen and sulfur belong to the same column in the Periodic Table, it is interesting to compare the effects of the two on CO diffusion on Ni(110). Similar to the S case, though not as strong, the effect of oxygen on CO diffusion can only be understood by an O-modified step-controlled diffusion model assuming O preferentially adsorbs at step sites. The observed increase of the apparent diffusion activation energy E_D versus θ_O for CO on Ni(110) cannot be explained by repulsive CO-O interaction on terraces, which leads to an opposite dependence of E_D on θ_O.[26,27] Diffusion of CO into the O-infected areas can explain qualitatively the increase of E_D versus θ_O, but it fails in quantitative agreement. At oxygen coverage of $\theta_O=0.15$ ML, for example, the CO diffusion coefficient was observed to have reduced by a factor of ~50 at ~180 K as compared to that on a clean Ni(110) surface. Simulation by Brand, Deckert, and George[11] for H diffusion on Ru(001), assuming that each surface impurity atom can block its ten nearest-neighbor and next-nearest-neighbor adsorption sites of H, predicts only a reduction of 11 in the diffusion coefficient at an impurity coverage of 0.15 ML. This reduction is already overestimated knowing that the oxygen poisoning range should not reach the next-nearest-neighbor sites.[28] The effect on CO diffusion due to diffusion of oxygen on terraces also would not explain our observation, since it can hardly occur in the temperature range of our measurement. Again, the oxygen-occupied step-controlled surface diffusion model appears most plausible. Such a model can explain quantitatively the observed experimental results presented in Fig. 4. Because it involves only some detailed changes of the fitting parameters as compared to the S case, we omit such a fit here. The fact that it requires a higher coverage of O than S to reach a similar effect on CO diffusion could be due to a smaller adsorption energy difference for oxygen on terraces and at step sites than that for S, making oxygen adsorption at step sites less favorable than S. This could be due to the fact that oxygen adsorbed on terraces can actually induce surface reconstruction, resulting in a lower energy difference between oxygen adsorption on terraces and at step sites.

It is known that, in contrast to the S case, adsorption of sufficient O impurities on terraces of Ni(110) can induce a surface reconstruction. STM and other studies have found that the reconstruction is in the form of added Ni rows along [001] via mass transportation of Ni from steps and adsorbed oxygen occupying the bridge sites of the added rows.[16,17,23] For $\theta_O<0.20$ ML, although CO molecules could also adsorb next to the added rows, most of them still occupy the short-bridge sites on the unreconstructed terraces.[19] The major effect of preadsorbed O is then in elimination of CO adsorption sites by the added Ni rows. Because of the low density of the O atoms that are away from the step sites, the density and average length of these added rows are small. Consequently, their effect on CO diffusion is expected to be weak. This is shown by the observation that E_D along [110] and [001] reach saturation at roughly the same oxygen coverage, although the added rows are along [001].

We also note that the saturation values of E_D in the cases of preadsorbed S and O are nearly the same. Whether this is a coincidence or not is difficult to answer.

C. CO/K on Ni(110)

Opposite to S and O, K is known as a promoter for Ni catalysis of CO hydrogenation.[3] It is therefore interesting to

know how differently K affects CO diffusion. At our flash annealing temperatures, adsorption of K at $\theta_K \sim 0.50$ ML on Ni(110) can induce a surface reconstruction, transforming it to $p(1\times 2)$ with missing Ni rows.[32] The missing Ni rows are along [110], perpendicular to the direction of the added Ni rows in the oxygen-induced reconstruction case. The K atoms are believed to adsorb in the troughs left by the missing Ni rows with no definite registry.[32] With partial K coverages, the K atoms presumably aggregate in local areas where surface reconstruction occurs. Because of strong attraction between CO and K,[21,33] the subsequently dosed CO molecules will first adsorb near K in the reconstructed areas. The adsorption site of CO near K is proposed to be the top site of the underlying second Ni layer (the first layer is formed by the remaining Ni rows).[32,34] A previous study suggests that each K atom can strongly interact with two nearest-neighbor CO molecules but relatively weakly with next-nearest-neighbor CO.[21] Thus at a potassium coverage θ_K, $2\theta_K$ of CO are strongly affected by K. The saturation CO coverage should also be reduced approximately by θ_K.[21,32] For example, at $\theta_K \sim 0.2$ ML, ~ 0.4 ML of CO should be strongly affected, which is half of the CO saturation coverage (~ 0.8 ML) at this θ_K. Therefore, unlike the S and O cases, CO molecules under direct influence of K are expected to contribute significantly to the observed CO diffusion.

Assuming that the K-CO attractive interaction only affects the adsorption sites but not the saddle points in the diffusion path, the energy barrier for CO diffusion near K is expected to increase to $E_a + \varepsilon_{\text{K-CO}}$, where E_a is the barrier energy on a clean surface and $\varepsilon_{\text{K-CO}}$ is the K-CO interaction energy, which is ~ 5.8 kcal/mol as deduced from thermal-desorption spectroscopy measurement.[33] If we assume that CO diffusion is determined by the K-attracted CO, then the effective energy barriers for CO diffusion along [110] and [001] should be $E_D = 8.0$ and 8.6 kcal/mol, respectively, knowing that $E_a = 2.2$ kcal/mol along [110] and $E_a = 2.8$ kcal/mol along [001]. These values of E_D appear to agree well with the measured saturation values of E_D at CO saturation coverage (see Fig. 6), although this could be fortuitous considering our starting assumption may not be valid.

The above picture is also difficult to explain the observed dependence of E_D on θ_K shown in Fig. 6. Along [010], CO diffusion has two parallel channels, one alongside the K-induced troughs and the other on terraces unaffected by K. Intuitively, this would not have led to an effective diffusion energy barrier linearly dependent on θ_K as observed. The mean-field model proposed by Zhdanov[27] may explain the relation, but it assumes an even distribution of K on the surface which is certainly not true in our case. Clearly a more sophisticated theory is needed to understand the experimental results. For CO diffusion along [001], the situation is even more complex, since the diffusion is now in the direction perpendicular to the K-induced troughs. The observed E_D versus θ_K is not linear as one would expect.

Several factors could have complicated the problem. First, the CO molecules adsorbed near K are at sites[31] different from those in the clean areas. They may have different values of E_a. Second, the K-induced reconstructed Ni rows may affect CO diffusion more drastically than we assume. Unlike S and O cases, CO molecules are attracted, instead of being repelled, to the K-induced reconstructed areas. This may have a significant effect. Third, how K-covered steps affect CO diffusion across the steps is not known. It is also not clear whether part of K impurities may have left on terraces to affect CO diffusion.

D. Comparison of the three surface impurities

CO diffusion on Ni(110) is sensitive to all three surface impurities, S, O, and K, although the situations are very different. The diffusion activation energy E_D in all cases increases with the impurity coverage, and approaches a saturation value of ~ 7–8 kcal/mol, relatively insensitive to the kind of impurities. For $\theta_{CO} = \theta_{Sat}$, the diffusion preexponential factor D_0 first increases with impurity coverage by about five orders of magnitude as E_D approaches saturation, but then decreases at higher impurity coverages. For $\theta_{CO} = 0.50$ ML, the behavior is similar; the increase of D_0 to its maximum is about two orders of magnitude.

The difference between the three impurity cases appears in the detailed impurity-coverage dependence of CO diffusion. With saturation CO coverage, it takes ~ 0.10 ML of S, ~ 0.15 ML of O, and ~ 0.20 ML of K to increase E_D to saturation. In the S case, high-temperature annealing further enhances the impurity effect for CO diffusing along [110]; only ~ 0.02 ML of S is needed to make E_D reach saturation. As discussed earlier, both S and O may have a higher probability to adsorb at step sites than on terraces, resulting in step-controlled diffusion of CO at sufficiently high impurity coverages. The stronger effect observed with S than O is presumably because S has a higher adsorption energy at step sites than O. However, the weaker effect from K is due to a different mechanism. It is the nearest-neighbor K-CO attractive interaction that seems to be responsible for slowing down the CO diffusion.

From our results, it is not surprising that S and O tend to poison the CO methanation reaction on Ni, since diffusion is a necessary step to bring CO and H together for CO to react with H on the surface. On the other hand, although K is known as a promoter for CO hydrogenations, it also strongly reduces CO diffusion on Ni(110) at relatively high K coverages. If diffusion is a limiting step for CO reactions, then it should have reduced the reactivity. Indeed, as reported by Campbell and Goodman,[3] K on Ni(100) does reduce the methane formation rate relative to clean Ni(100). The reason for reduction of the methanation rate was speculated to be due to K poisoning the adsorption of the other reactant, i.e., hydrogen. We now suspect that slowing down of CO diffusion by K is responsible for the decrease.

E. Dependence on CO coverage and directions of diffusion

For both S and O preadsorbed Ni(110) surfaces, we found that the activation energy E_D for CO diffusion reaches its saturation value at a higher impurity coverage for $\theta_{CO} \sim \theta_{Sat}$ than for $\theta_{CO} \sim 0.5$ ML. The value of saturation E_D, however, is about the same.

On a clean Ni(110) surface, it is known that CO-CO interaction is responsible for the coverage dependence of CO diffusion.[35] The same can be used to explain the above finding. In the impurity-modified step-controlled diffusion model

for S and O, the CO molecules have two channels to cross over an impurity modified step: direct across an impurity-covered step site, or via a detour around the impurity-covered part of the step. At a given impurity coverage, the latter channel contributes relatively more to D_s in Eq. (3) for $\theta_{CO} \sim \theta_{Sat}$ than for $\theta_{CO} \sim 0.5$ ML, since the repulsive CO-CO interaction can lower the diffusion barrier on terraces and speed up CO diffusion on terraces more for $\theta_{CO} \sim \theta_{Sat}$ than for $\theta_{CO} \sim 0.5$ ML.[36] This makes the detour diffusion around impurity-occupied steps more important for $\theta_{CO} \sim \theta_{Sat}$; the step-controlled diffusion becomes dominating only when the steps are almost all covered by impurities. For $\theta_{CO} \sim 0.5$ ML, the step-controlled diffusion is expected to set in at a lower impurity coverage.

Anisotropy of CO diffusion on Ni(110) was found to be greatly reduced by preadsorbed impurities. At $\theta_{CO} \sim \theta_{Sat}$, with preadsorbed S, E_D has a saturation value of 7.4 kcal/mol for CO diffusing along $[1\bar{1}0]$, and 7.8 kcal/mol for CO diffusing along [001]. For the case of preadsorbed O, the saturated values of E_D are 8.5 and 7.9 kcal/mol for diffusion along $[1\bar{1}0]$ and [001], respectively. The reduced anisotropy is certainly a reflection of the impurity-controlled diffusion process. That makes the apparent activation energy barrier nearly the same.

V. SUMMARY

We have studied experimentally the impurity effects on CO diffusion on Ni(110). A few percent of a monolayer of preadsorbed S, O, and K can drastically reduce the CO diffusion rate in decreasing order from S to O to K. In the S case, annealing of the sample at high temperature can make the impurity effect more pronounced, due to a step morphology change. With both S and O, impurity-covered steps appear to be responsible for impeding the CO diffusion. A model calculation based on the impurity-modified step-controlled diffusion mechanism can explain the experimental data well. In the case of K, the mechanism for impeding CO diffusion on Ni(110) seems to originate from nearest-neighbor interaction between K and CO rather than from step control. Our findings here suggest that for intrinsic surface diffusion studies to be reliable, it is important to keep the surface very clean. They also suggest that we must not underestimate the role of an impurity in discussing the inconsistent results reported in the past on nominally identical systems. The observed impurity effect on CO diffusion may be directly connected to the impurity poisoning effect on CO catalytic reactions.

ACKNOWLEDGMENTS

The authors gratefully acknowledge Professor S. C. Ying for fruitful discussions. X.-D.X. acknowledges the support from the Research Grants Council of Hong Kong, Grant No. HKUST684/96P. This work was supported by the Director, Office of Energy Research, Office of Basic Energy Sciences, Materials Sciences Division of the U.S. Department of Energy under Contract No. DE-ACO3-76SF00098.

[1] For example, see a review by R. Gomer, Rep. Prog. Phys. **53**, 917 (1990).

[2] S. Esch, M. Hohage, T. Michely, and G. Comsa, Phys. Rev. Lett. **72**, 518 (1994).

[3] C. T. Campbell and D. W. Goodman, Surf. Sci. **123**, 413 (1982), and references therein.

[4] R. Lewis and R. Gomer, Nuovo Cimento Suppl. **5**, 506 (1967); B. Poelsema, L. K. Verheij, and G. Comsa, Phys. Rev. Lett. **49**, 1731 (1982); J. E. Reutt-Robey, D. J. Doven, Y. J. Chabal, and S. B. Christman, *ibid.* **61**, 2778 (1988); J. Chem. Phys. **93**, 9113 (1990); V. J. Kwasniewski and L. D. Schmidt, Surf. Sci. **274**, 329 (1992); H. Froitzheim and M. Schulze, *ibid.* **320**, 85 (1994).

[5] S. M. George, A. M. Desantolo, and R. B. Hall, Surf. Sci. **159**, L425 (1985); D. A. Mullins, B. Roop, and J. M. White, Chem. Phys. Lett. **129**, 511 (1986); T.-S. Lin and R. Gomer, Surf. Sci. **255**, 41 (1991); X. D. Zhu, A. Lee, and A. Wong, Phys. Rev. Lett. **68**, 1862 (1992).

[6] M. C. Tringides, Surf. Sci. **204**, 345 (1988); J. Chem. Phys. **92**, 2077 (1990); M. C. Tringides and R. Gomer, Surf. Sci. **265**, 283 (1992).

[7] H. Roux, A. Piquet, R. Uzan, and M. Drechsler, Surf. Sci. **59**, 97 (1976); H. Roux, A. Piquet, G. Pralong, R. Uzan, and M. Drechsler, *ibid.* **71**, 375 (1978).

[8] M. Pichaud and M. Drechsler, Surf. Sci. **32**, 341 (1972); **36**, 813 (1973).

[9] J. Perdereau and G. E. Rhead, Surf. Sci. **7**, 175 (1967); F. Delamare and G. E. Rhead, *ibid.* **28**, 267 (1971).

[10] R. Morin and M. Drechsler, Surf. Sci. **111**, 140 (1981).

[11] J. L. Brand, A. A. Deckert, and S. M. George, Surf. Sci. **194**, 457 (1988); C. H. Mak, B. G. Koehler, J. L. Brand, and S. M. George, J. Chem. Phys. **87**, 2340 (1987).

[12] Xu-Dong Xiao, Yuanlin Xie, Christian Jakobsen, Heather Galloway, Miquel Salmeron, and Y. R. Shen, Phys. Rev. Lett. **74**, 3860 (1995).

[13] Xu-dong Xiao, X. D. Zhu, W. Daum, and Y. R. Shen, Phys. Rev. B **46**, 9732 (1992).

[14] Xu-dong Xiao, Yuanlin Xie, and Y. R. Shen, Surf. Sci. **271**, 295 (1992).

[15] D. R. Huntley, Surf. Sci. **240**, 13 (1990).

[16] F. Besenbacher, I. Stensgaard, L. Rusan, J. K. Norskov, and K. W. Jacobsen, Surf. Sci. **272**, 334 (1992).

[17] B. Voigtlander, S. Lehwald, and H. Ibach, Surf. Sci. **225**, 162 (1990).

[18] H. Bu, C. D. Roux, and J. W. Rabalais, J. Chem. Phys. **97**, 1465 (1992).

[19] C. S. Feigerle, S. H. Overbury, and D. R. Huntley, J. Chem. Phys. **94**, 6264 (1991).

[20] R. L. Gerlach and T. N. Rhodin, Surf. Sci. **19**, 403 (1970).

[21] Lloyd J. Whitman and W. Ho, J. Chem. Phys. **83**, 4808 (1985).

[22] M. Blaszczyszyn, R. Blaszczyszyn, R. Meclewski, A. J. Melmed, and T. E. Madey, Surf. Sci. **131**, 433 (1983).

[23] P. Sprunger, F. Besenbacher, I. Stenstgaard, and E. Lægsgaard, Surf. Sci. **320**, 271 (1994).

[24] John L. Gland, Rober J. Madix, Robert W. McCabe, and Craig DeMaggio, Surf. Sci. **143**, 46 (1984); R. J. Madix, Michael Thornburg, and S.-B. Lee, *ibid.* **133**, L447 (1983); E. L.

Hardegree, Pin Ho, and J. M. White, *ibid.* **165**, 488 (1985).
[25] M. Trenary, K. J. Uram, and J. T. Yates, Jr., Surf. Sci. **157**, 512 (1985).
[26] David A. Reed and Gert Ehrlich, Surf. Sci. **102**, 588 (1981).
[27] V. P. Zhdanov, Phys. Lett. A **137**, 225 (1989).
[28] P. J. Feibelman, Annu. Rev. Phys. Chem. **40**, 261 (1989); P. J. Feibelman and D. R. Hamann, Phys. Rev. Lett. **52**, 61 (1984); Surf. Sci. **149**, 48 (1985); J. M. Maclaren, J. B. Pendry, and R. W. Joyner, *ibid.* **165**, L80 (1986); **178**, 856 (1986); J. M. Maclaren, J. B. Pendry, R. W. Joyner, and P. Meehan, *ibid.* **175**, 263 (1986); E. Wimmer, C. L. Fu, and A. J. Freeman, Phys. Rev. Lett. **55**, 2618 (1985); J. K. Norskov, S. Holloway, and N. D. Lang, Surf. Sci. **137**, 65 (1984); N. D. Lang, S. Holloway, and J. K. Norskov, *ibid.* **150**, 24 (1985).
[29] The diffusion energy barrier at a clean step site is ~5.5 kcal/mol, larger than that on the terrace. However, due to compensation from the preexponential factor, the diffusion coefficient over such a step site is comparable to that on the terrace over the temperature range of our interest.
[30] $L_0 \sim 1300$ Å along $[1\bar{1}0]$ and ~600 Å along [001] were computed from the miscut ~0.2° along the direction about 25° from $[1\bar{1}0]$, as manifested by STM images showing ~20 steps/μm, $\sim\frac{2}{3}$ of which were along the miscut direction, $\sim\frac{1}{6}$ along $[1\bar{1}0]$, $\sim\frac{1}{30}$ along [001], and $\sim\frac{1}{7}$ along the diagonals of the surface unit cells.
[31] J. Merikoski and S. C. Ying, Surf. Sci. Lett. **381**, L623 (1997).
[32] P. Statiris, P. T. Haberle, and T. Gustafsson, Phys. Rev. B **47**, 16 513 (1993); D. K. Flynn, K. D. Jamison, P. A. Thiel, G. Ertl, and R. J. Behm, J. Vac. Sci. Technol. A **5**, 794 (1987).
[33] A. Ramirez Cuesta and G. Zgrablich, Surf. Sci. **275**, L636 (1992).
[34] D. A. Wesner, F. P. Coenen, and H. P. Bonzel, Phys. Rev. Lett. **60**, 1045 (1988).
[35] Xudong Xiao, Yuanlin Xie, and Y. R. Shen, Phys. Rev. B **48**, 17 452 (1993).